



Attribution of recent warming in Alaska

John E. Walsh*, Brian Brettschneider

International Arctic Research Center, University of Alaska, Fairbanks, AK, USA



ARTICLE INFO

Keywords:

Climate trends
Attribution
Atmospheric circulation
Alaska

ABSTRACT

Alaska has experienced some of the strongest warming rates in the Northern Hemisphere since the mid-20th century. The winter-season warming is especially strong: approximately 4.1 °C since 1950. The atmospheric circulation contributes to interannual variability of Alaska's temperatures through advection and thereby contributes to temperature trends over decadal to multidecadal timescales. In this study, we quantify the contribution of the atmospheric circulation to Alaska's warming by using an analog methodology to identify years with sea level pressure patterns most closely resembling the pressure pattern of each year between 1950 and 2017. The analogs enable a dynamical adjustment of temperature anomalies by removing the contribution of the atmospheric circulation. The dynamical adjustment explains approximately half the variance of Alaska's statewide temperature in winter, and smaller fractions in the other seasons. The unexplained variance, termed the “excess warmth,” shows a systematic increase from 1950 to 2017. The trends in the excess warmth correspond to a warming of 2.1 °C in winter and spring, 1.3 °C in summer, and 0.5 °C in autumn, which are consistent with the trends simulated by global climate models run with historical and projected greenhouse gas concentrations for the same period. The excess warmth accounts for 51% of the Alaska's winter warming and 75% of Alaska's annual mean warming over the 1950–2017 time period.

1. Introduction

Recent changes in the Arctic's climate have been large and widely reported (SWIPA, 2011; IPCC, 2013; Overland et al., 2018). These changes span multiple components of the climate system: sea ice, snow cover, glaciers and the Greenland Ice Sheet, and permafrost. Changes in these various components are consistent with a warming atmosphere, which has also been well documented, especially during the past several years when the Arctic has reached new records for winter and annual temperatures (Richter-Menge and Mathis, 2017). While greenhouse gases have been implicated in the warming and its impacts on the cryosphere, little work has been done to quantify the anthropogenic contribution as a fraction of the overall warming. The present paper represents a step towards this quantification by evaluating the contribution of changes in atmospheric circulation in a region (Alaska) for which the warming of recent decades is typical of the Arctic.

Fig. 1 shows the post-1950 Arctic warming of the Arctic's annual (January–December) and winter season (December–February) temperatures. We choose 1950 as the starting date because of the availability of corresponding reanalysis output with reliable sea level pressure fields for Alaska and the surrounding area; these fields provide the basis for the analog methodology described in Section 2. Alaska's

annual mean warming, which is slightly more than 2 °C since 1950, is typical of most of the Arctic (Fig. 1a). The Arctic's warming is greater than most of the rest of the Northern Hemisphere, a manifestation of the well-known Arctic amplification (e.g., Pithan and Mauritsen, 2014). However, the Arctic's winter warming (Fig. 1b) shows a spatially more complex pattern, with a maximum over Alaska, northwestern Canada and the Beaufort Sea. The greater spatial complexity of the winter pattern is consistent with a greater role of the atmospheric circulation in advecting into a region air that is warmer or colder than the region's climatological mean. The atmospheric circulation has a large component of internal variability, and variability of the atmospheric (and oceanic) circulation is indeed one of the major sources of uncertainty in climate trends over decadal to multidecadal timescales (Hodson et al., 2013; Shepherd, 2014; Deser et al., 2014).

While in situ measurements of temperature are sparse over marine areas of the Arctic, Alaska has a network of surface stations with relatively complete records of temperature back to the late 1940s. These stations are not evenly distributed: coastal and southern regions of the state have denser coverage (Bieniek et al., 2012). However, the relatively good station coverage together with the Arctic-wide representativeness of Alaska's annual mean warming make Alaska an attractive regional test case for a diagnostic evaluation of the drivers of Arctic

* Corresponding author. International Arctic Research Center, University of Alaska, Fairbanks, AK 99775, USA.
E-mail address: jewalsh@alaska.edu (J.E. Walsh).

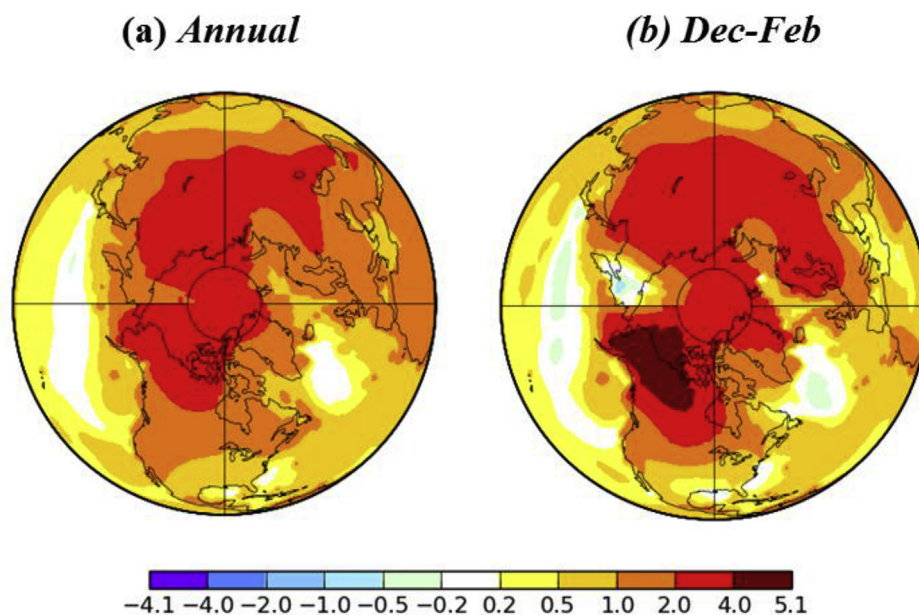


Fig. 1. Surface air temperature change ($^{\circ}\text{C}$) from 1950 to 2017 based on least-squares linear fit to (a) annual and (b) winter temperatures. Source: NASA Goddard Institute for Space Studies, <https://data.giss.nasa.gov/gistemp/maps/>, accessed 5 September 2018.

temperature variations and trends.

Internal variability is readily apparent in the annual temperatures at the regional scale. Fig. 2 shows time series of the annual and winter (December–February) statewide average temperatures for Alaska for the 1950–2017 period. While positive trends are apparent in both time series, interannual and multiyear variations are large, and in some cases the interannual variations are larger than the overall trend for the 68-year period. The 68-year changes based on least-squares fits to the time series in Fig. 2 are 4.1°C for winter and 2.1°C for the annual values. The corresponding trend-derived changes for the other seasons (not shown) are 2.2°C for spring, 1.3°C for summer and 0.8°C for autumn, indicating that the warming has been largest in winter and smallest in autumn. For comparison, the standard deviations of the seasonal temperatures are 4.4°C for winter, 3.1°C for spring, 1.4°C for summer, 2.6°C for autumn, and 2.1°C for the annual temperatures, indicating that interannual variability is still large relative to the overall seasonal trends over the 68-year period.

An underlying premise of this paper is that the interannual variations and trends in Fig. 2 are attributable, at least in part, to variations in the atmospheric circulation. Interannual temperature variations over Alaska and northwestern Canada have been tied to variations of large-scale modes of variability such as the Pacific Decadal Oscillation (Hartmann and Wendler, 2005; McAfee, 2014) and the El Niño/Southern Oscillation (Papineau, 2001), which include teleconnected anomalies of sea level pressure that drive the near-surface wind anomalies. The jump in Alaskan temperatures in the late 1970s, apparent in Fig. 2, has been attributed by Hartmann and Wendler to a change of phase of the Pacific Decadal Oscillation. Indeed, the statewide average temperature for the 20 years following the 1977–78 shift exceeded average temperature of the preceding 20 years by 1.6°C in winter and 1.0°C in the annual mean. These changes represent substantial portions, although less than half, of the overall changes of 4.1°C and 2.1°C in the winter and annual temperatures during our study period. It should be noted, however, that the stationarity of large-scale teleconnections affecting Alaska is open to question. McAfee (2014), for example, shows that the relationships between the Pacific Decadal Oscillation and Alaskan temperatures are variable over time.

The atmospheric circulation over Alaska is controlled largely by the Aleutian low pressure system during winter (Shulski and Wendler, 2007), as shown by the climatological mean pattern of

December–February sea level pressure (Fig. 3a). Papineau (2001) and Mills and Walsh (2013) showed that large-scale modes of atmosphere-ocean variability have significant effects on Alaska's temperatures, especially in the cold season. The Aleutian low varies in intensity and location from one year to the next. The Pacific Decadal Oscillation and ENSO contribute to these variations. During summer, Alaska is on the northern fringes of the pressure gradient associated with the Pacific subtropical high (Fig. 3b), although migratory synoptic systems result in a weak gradient in the mean sea level pressure field over central and northern Alaska. Interannual variations in the atmospheric circulation are manifestations of the internal variability, which is a major contributor to trends over multiyear and multidecadal timescales (Deser et al., 2014).

Two of the most recent winters (2015–16 and 2016–17) in Fig. 2b provide support for the premise that the atmospheric circulation is a key factor in interannual temperature variations over Alaska. The statewide average temperatures for December–February ending in 2016 and 2017 were -9.8°C and -14.7°C , respectively. These temperatures represent departures of $+4.7^{\circ}\text{C}$ and -0.2°C from the mean for the 1980–2010 reference period currently in use by the National Weather Service. The difference of approximately 5°C in the 3-month mean temperatures is consistent with the sea level pressure anomalies for the same three-month periods. Fig. 4 shows that the 2015–2016 winter was characterized by negative pressure anomalies of more than 12 hPa in the Aleutian region, corresponding to an unusually deep Aleutian low with anomalous northward airflow and warm advection into mainland Alaska. By contrast, the winter of 2016–17 had positive sea level pressure anomalies of more than 10 hPa in the Aleutians, with even larger anomalies to the south, contributing to the eastward advection of cold air from Siberia into much of Alaska. The sensitivity of Alaskan temperatures to near-surface atmospheric circulation, illustrated by the temperature and sea level pressure anomalies of these two recent winters, leads to the hypothesis that much of the trend of winter (and annual) temperatures over Alaska during recent decades is attributable to variations of the atmospheric circulation.

The quantification of the role of the atmospheric circulation in trends of temperature is not new, and previous work has used the term “dynamical adjustment” to account for the effect of the atmospheric circulation on trends of temperature. Circulation analogs, which are at the core of the dynamical adjustment approach used in this study, were

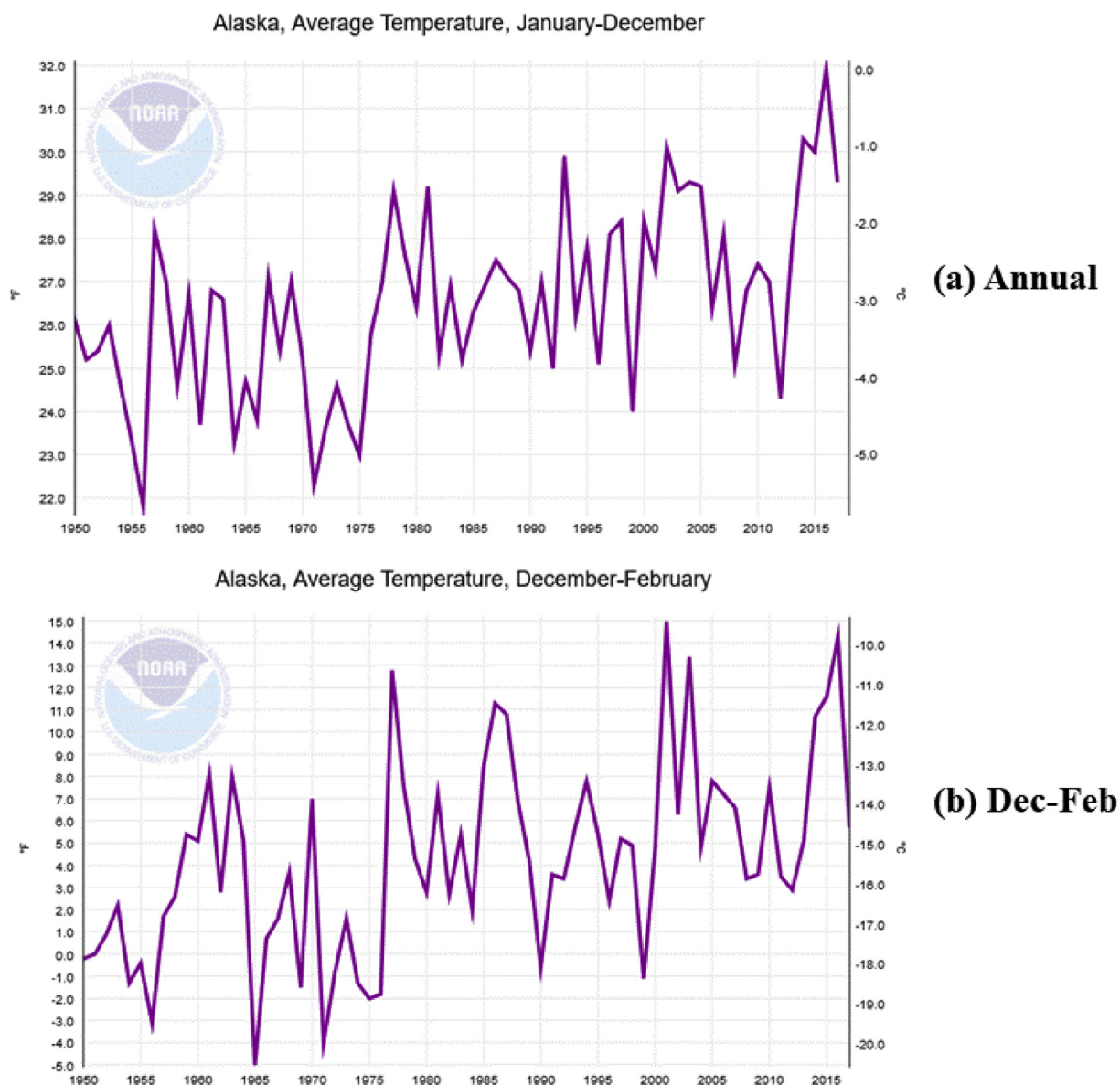


Fig. 2. Time series of Alaska statewide temperature for 1950–2017 for the full calendar year (upper panel) and for winter (lower panel). Temperature scales for °C and °F are shown on the right and left ordinate axes, respectively. Source: National Centers for Environmental Information, <https://www.ncdc.noaa.gov/cag/>, accessed 5 September 2018.

introduced into the study of atmospheric predictability by Lorenz (1969) and into seasonal prediction by Van den Dool et al. (2003). Cattiaux et al. (2010) applied an analog approach to dynamically adjust temperature trends over Europe. More recently, Deser et al. (2016) applied a similar approach to evaluate the contribution of the atmospheric circulation to wintertime trends of temperature over North America. While Deser et al.’s results were limited to the winter season, they showed that internal variations of the atmospheric circulation in an ensemble of climate model simulations explained about one-third of the winter temperature trend over North America during 1963–2012. Notably for this study, the dynamical adjustment reduced the trends over Alaska and northwestern Canada by about 40% (Deser et al., 2016, Table 1 and Fig. 7). In a more recent application of the analog-based method, dynamical adjustment has also been found to advance the time of emergence of the signal of externally forced climate change over North America and Europe in both summer and winter (Lehner et al., 2017).

Other dynamic adjustment procedures have led to similar conclusions about the importance of the atmospheric circulation for monthly

and seasonal temperature anomalies and associated trends. Smoliak et al. (2015) used a partial-least-squares regression technique to show that dynamical adjustment accounts for about half of the variance of monthly temperatures over Northern Hemisphere land areas during the cold season. In an application to Europe using five different versions of the dynamic adjustment procedure, Saffioti et al. (2017) found that dynamical adjustment also accounts for a substantial portion of the uncertainty in trends of winter (Dec–Feb) temperature and precipitation over Europe regardless of the procedure used.

With these large-scale studies as background, the present work focuses on Alaska as a case study for the impact of the atmospheric circulation on the variability and trends of air temperature. We distinguish our study from the growing literature on dynamical adjustment by performing an evaluation that includes all four seasons. Our main objectives are to show how the atmospheric circulation has impacted Alaskan temperature trends during a period when Alaska has emerged as a “hot spot” in the global warming story, to determine how much of the warming is attributable to factors other than the atmospheric circulation, and to document the seasonality of the portion of the warming

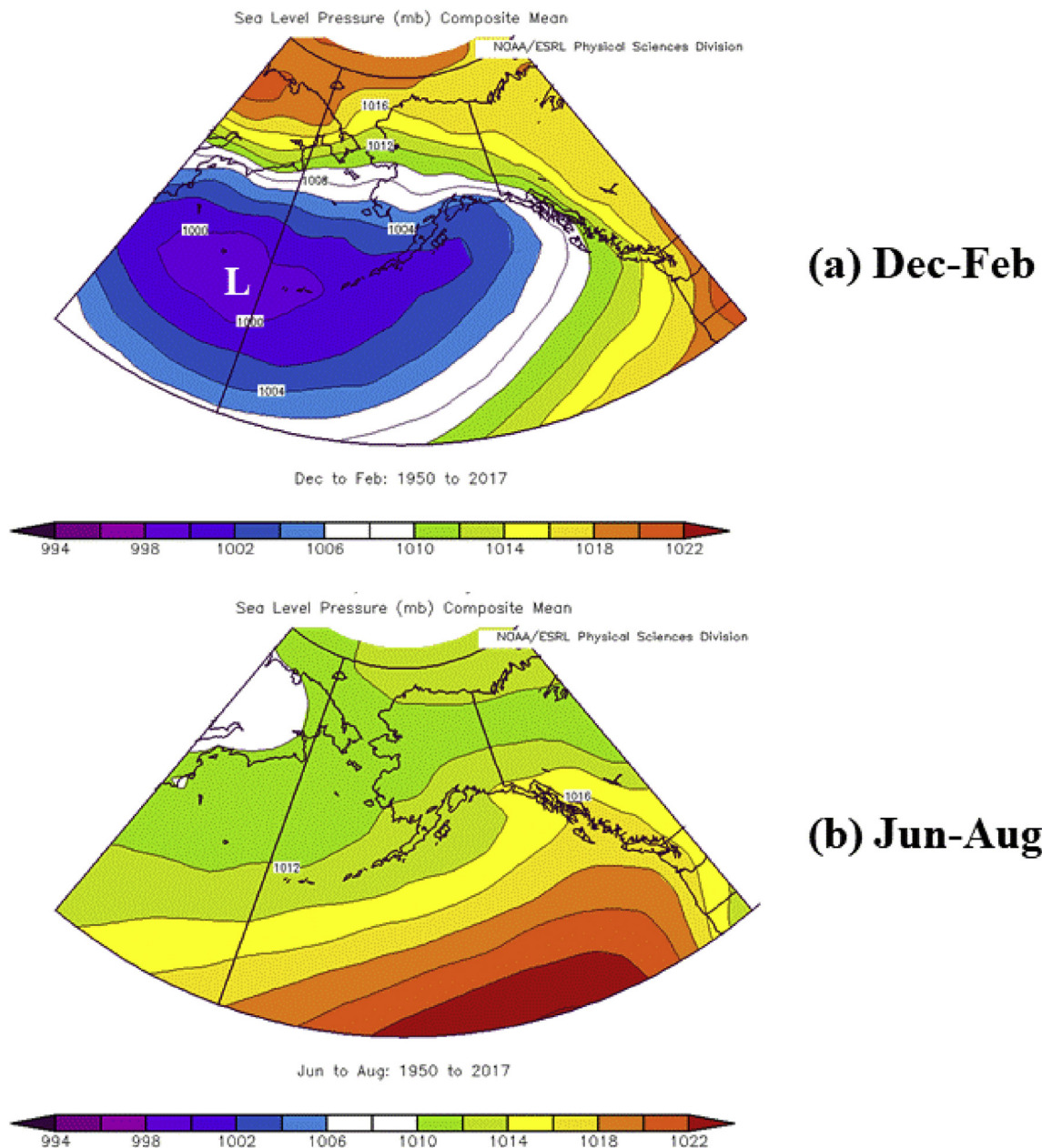


Fig. 3. Mean (1950–2017) sea level pressures (hPa) over Alaska and surrounding region for (a) winter, Dec–Feb and (b) summer, Jun–Aug. Contour interval (2 hPa) and color bar are the same for both panels. (For interpretation of the references to color in this figure legend, the reader is referred to the Web version of this article.)

that is not associated with the atmospheric circulation.

2. Data and methods

The primary data sets used in this study are (1) Alaska station temperatures grouped into climate divisions (Bieniiek et al., 2012) by the National Centers for Environmental Information (<https://www.ncdc.noaa.gov/cag/statewide/time-series>, accessed 5 September 2018) and (2) sea level pressures from the NCEP/NCAR reanalysis (Kalnay et al., 1999) archived at the Earth System Research Laboratory of the National Oceanic and Atmospheric Administration (<https://www.esrl.noaa.gov/psd/cgi-bin/data/composites/printpage.pl>, accessed 5 September 2018). The statewide temperatures are monthly and date back to 1925, although only the values from December 1949 onward are used here for compatibility with the available data on sea level pressure. We use the monthly temperatures to compute seasonal values using the conventional definitions of the seasons (winter = Dec–Feb,

spring = Mar–May, summer = Jun–Aug, autumn = Sep–Nov). The re-analysis-based sea level pressure fields, which are available at 6-hourly intervals back to 1949, are also converted to seasonal means for each year.

Our diagnostic evaluation of the contribution of the atmospheric circulation to the recent warming of Alaska is based on an analog methodology. The analog methodology was illustrated for a single year by Walsh et al. (2017), who showed that winds accounted for a substantial portion of the anomalous warmth of the 2015–16 cold season (October–April). The approach consists of a comparison of a particular year's sea level pressure (SLP) field over the Alaska region (50°–75°N, 130°–180°W) with the SLP fields of all other years in the 1949–2017 period, the selection of the five years with the closest match of SLP fields, and the construction of an analog-derived temperature by averaging the temperatures of the five best analog years. Walsh et al. (2017) documented sensitivities of the procedure to the size of the domain used for analog selection, the metric of similarity (root-mean-square

Departures from 1981–2010 mean sea level pressure (Dec–Feb)

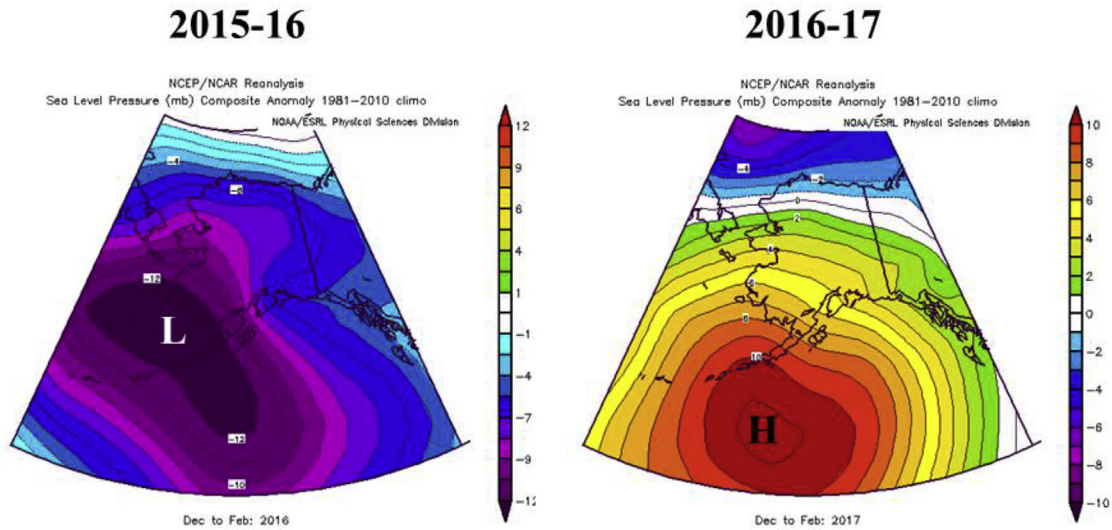


Fig. 4. Departures from climatological mean (1981–2010) sea level pressure (hPa) for December–February of 2015–16 (left) and 2016–17 (right). Contour interval (2 hPa) and color bar are the same for both panels. (For interpretation of the references to color in this figure legend, the reader is referred to the Web version of this article.)

Table 1

Correlation between observed Alaska statewide temperature and corresponding temperatures of best analog years as a function of N, the analog number (N = 1 is the best analog, N = 2 is second best, ..., N = 5 is fifth best).

	Analog number				
	1	2	3	4	5
Dec–Feb	.71	.58	.39	.40	.35
Mar–May	.44	.32	.14	.20	.16
Jun–Aug	.15	.18	.12	.14	.05
Sep–Nov	.02	.25	.28	.16	.32

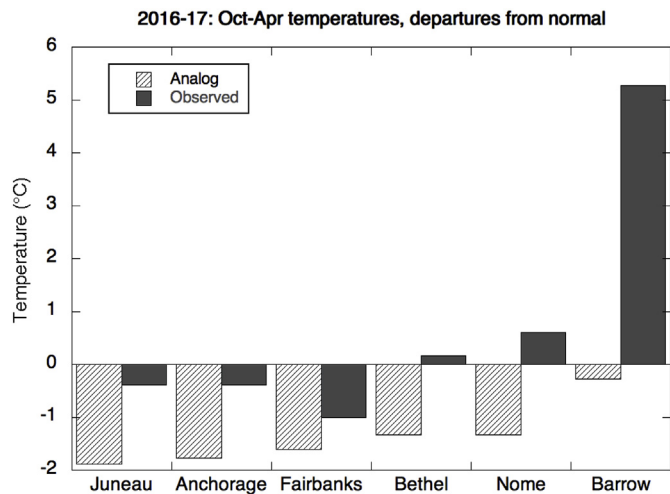


Fig. 5. Observed temperatures (solid bars) and average temperatures of the five best analog years (hatched bars) for the October–April period of 2016–2017.

difference vs. spatial pattern correlation), the variable used for the analog selection (SLP, upper-air geopotential height), and the number of analogs that were averaged (1, 2, ..., 10). Guided by the results in the previous study, we base our analog-year selection in this study on the spatial pattern correlation over the Alaska domain bounded by 50°N,

75°N, 180°W and 130°W), SLP as the analog selection variable, and the five best analogs for each year. We perform the analog selection separately of each season.

As noted in the preceding section, analog methodologies have been used by other investigators to evaluate the atmospheric circulation's contribution to temperature variations and trends. The cited studies by Cattiaux et al. (2010), Deser et al. (2016) and Lehner et al. (2017) used a procedure in which “constructed analogs” were derived as weighted combinations of the best analogs in order to optimize the correspondence between sea level pressure patterns and air temperatures. The present study uses a variant of this approach by applying equal weights to the (five) best analogs for a particular month. We choose this approach rather than an uneven weighting because sensitivity studies in our previous work with analogs found that the correlations with air temperature showed only a weak dependence on the number, N, of composited analogs, when N was increased from 1 to 10 (Walsh et al., 2017, Table 1).

3. Results

As an example of the analog-derived specifications, we apply the procedure to the 2016–2017 cold season (October–April), which followed the warmest cold season (2015–2016) in Alaska's historical record. Temperatures over the 2016–2017 cold season averaged close to the long-term mean over most of the state, as shown in Fig. 5 for the cities of Juneau, Anchorage, Fairbanks, Bethel and Nome. However, temperatures were well above normal (by more than 5 °C) at Barrow on Alaska's northern coast. Fig. 5 shows that the analog-derived temperatures for the 2016–17 cold season were colder than the observed temperatures at all six locations. The below-normal temperatures of the analog years, which were the years with sea level pressure patterns most closely matching Fig. 4b, are consistent with the relatively cold advection implied by Fig. 4b. The difference (observed minus analog-derived) was 1°–2 °C at all locations except Barrow, where the analog-derived value of –0.2 °C was far below the observed temperature. The implication is that non-dynamic factors contributed to the warmth of 2016–17 relative to the past years that were the best analogs. In the case of Barrow, the loss of sea ice, manifest as thinner ice and more

Correlation: Actual vs. Analog-derived T

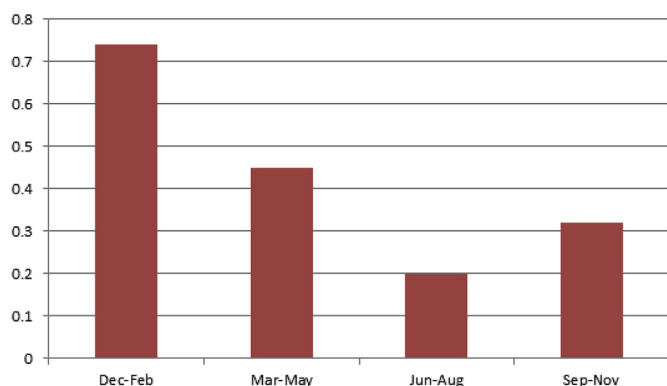


Fig. 6. Correlations between seasonal temperature and the mean temperature of the five best analog years.

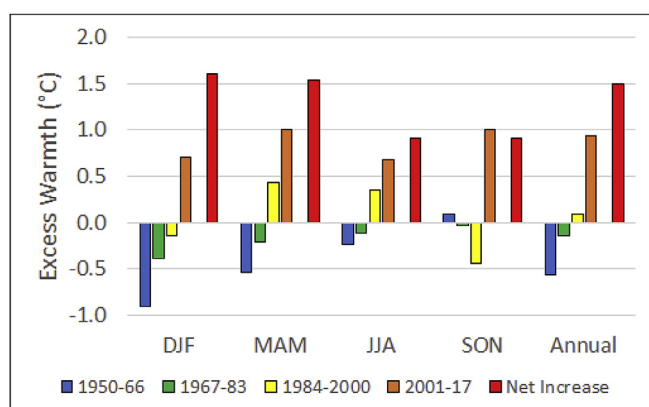


Fig. 7. Excess warmth (°C) by season and quartile (17-year period), from earliest (blue) to most recent (orange). Negative values indicate that actual temperature was cooler than the analog-derived, positive values indicate actual temperature was warmer than analog-derived. Also shown (red bars) are the total changes in excess warmth from the first to the last quartile. (For interpretation of the references to color in this figure legend, the reader is referred to the Web version of this article.)

open water than in the past, is the prime candidate for the explanation of the remarkable temperature anomaly (5.3 °C) relative to the remainder of the stations (and the statewide average anomaly, which was only 0.2 °C for the October–April period). The smaller increments of warmth at the other locations are consistent with the greenhouse gas forcing that is addressed later in this paper.

In order to illustrate quantitatively the level of correspondence between each year’s SLP fields and the statewide mean temperature, Fig. 6 shows, for each season, the correlations of the yearly statewide temperature for that season with the mean seasonal temperature of the corresponding five best SLP analog years. In all seasons, the 5-analog mean temperature correlates more highly with the actual temperature than does the single best (or any other) analog, although the incremental gain by adding additional analogs beyond the first- or second-best is small (Table 1). As shown in Fig. 6, the correlations between the 5-analog mean and the actual temperatures range from 0.74 in winter (DJF) to 0.20 in summer (JJA), indicating that the atmospheric circulation as represented by SLP explains 55% of the variance in winter but only 4% of the variance in summer, with the values for the transition seasons falling in between. This result makes sense synoptically because temperature gradients in the Alaska region are largest in winter and smallest in summer, so advection by winds is more effective in creating temperature anomalies in winter than in summer. In addition, pressure

gradients and winds are stronger in winter than in summer, as shown by the mean SLP fields for DJF and JJA in Fig. 3.

For the remainder of the study, we use the temperature anomaly averaged over the five best analog years as a metric of the atmospheric circulation’s contribution to a particular year’s temperature anomaly in each season. The portion of the temperature anomaly unexplained by the atmospheric circulation then becomes the focus of our analysis. The portion of a seasonal temperature anomaly unexplained by the atmospheric circulation can be attributable to (1) local effects that aggregate systematically in a statewide average, (2) anomalous surface states (anomalies of ocean temperature, sea ice, snow cover), or (3) external forcing such as the effects of increasing greenhouse gas concentrations. A clean separation of the second and third potential attribution sources is not possible from the observational data because increasing greenhouse gas forcing can result in changes in ocean temperature, sea ice and/or snow cover, thereby augmenting direct radiative effects on air temperature. The direct radiative effects of increasing greenhouse gas concentrations may be further partitioned into increased downwelling radiation from anthropogenic sources (CO₂, CH₄, etc.) and from water vapor, as atmospheric warming is expected to be accompanied by an increase of specific humidity (Serreze et al., 2012; Cullather et al., 2016). However, if the temperature anomaly unexplained by the atmospheric circulation shows a systematic warming over time, then one can point to a trend of “excess warmth” that is consistent with the direct and indirect effects of increasing greenhouse gas concentrations.

In the following summary of the results for the entire 1950–2017 period, “excess warmth” will refer to the differences between the actual and dynamically adjusted seasonal temperatures. This “excess warmth” will be negative if the actual temperature is colder than the mean value of the five best circulation analog years, and it will be positive if the actual temperature is warmer than the analog-derived value. Fig. 7 shows the excess warmth as a function of season and subperiod (quartile) of the 68-year period of record. In all seasons except autumn, the excess warmth increases monotonically from the earliest to the most recent 17-year quartile. In all seasons but autumn, it is negative in the first two quartiles and positive in the two most recent quartiles. Even in autumn, the most recent quartile has the most positive value of excess warmth. The increase from the first to the final quartile ranges from 1.2 °C in autumn to 3.0 °C in winter, with an annual mean increase of 1.5 °C. As an indication of the sensitivity to the metric used in analog selection, we note that the winter-season increase of excess warmth is 3.0 °C when analogs selection is based on the spatial pattern correlation, while it is 4.1 °C when based on the root-mean-square difference of the gridded pressures.

Least-squares linear fits to the time series of excess warmth for each season enable estimates of changes from 1949 to 50 to 2016–17. These changes are shown in Fig. 8, together with the corresponding total changes in temperature computed from the trends of temperature that include the circulation-driven component. Fig. 8 also shows the percentages of the total trend that the excess warmth represents in each season. During winter the linear-trend increase of excess warmth is approximately 2.1 °C, which is 51% of the total linear-trend-derived change of 4.2 °C. During autumn, the 0.5 °C linear increase of excess warmth represents 64% of the total warming. During spring and summer, nearly all the total increase of temperature is “excess warmth”, as there is essentially no trend in the circulation-derived component of the temperatures. Alternatively, one may say that the atmospheric circulation has not made a detectable contribution to changes of temperature over Alaska during spring and summer, while it has made a substantial contribution in winter and autumn. In the terminology of previous attribution studies, the temperature trend has a dynamically forced component in winter and autumn, but not in spring and summer. If the values for the four seasons are averaged into annual values, the increase of excess warmth is 1.5 °C, which is approximately 75% of the overall 2.1 °C increase of annual mean temperature from 1950 to 2017. However, it should be emphasized that this percentage has a strong

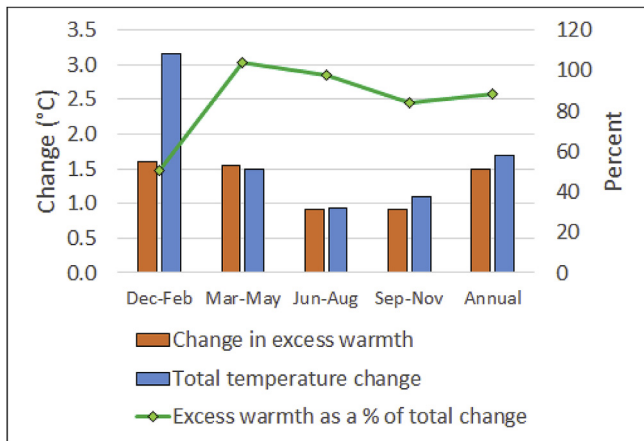


Fig. 8. Change in excess warmth by season based on least-squares linear fit to yearly values, 1949/50 through 2016/17 (blue bars). Also shown are total changes of temperature (red bars) and change in excess warmth as a percentage of the total change of temperature (green line). The latter is the same as the ratio of the trends. (For interpretation of the references to color in this figure legend, the reader is referred to the Web version of this article.)

seasonal variation. Winter and autumn are the seasons in which the atmospheric circulation has been a major contributor (49% in winter, 36% in autumn) to the overall temperature trend.

The change in excess warmth over time may be regarded as the dynamically adjusted temperature trend. Fig. 9 shows the spatial distribution of this trend, expressed as the difference in excess warmth

between the first and fourth quartiles, for each season in each of Alaska's 13 climate divisions (Bieniek et al., 2012). Consistent with the changes in the statewide averages in Figs. 7 and 8, the trend in excess warmth is largest during winter and spring in most of the climate divisions. However, there is little seasonality in the southeastern divisions, and the northernmost (North Slope) division shows a larger increase in autumn than in spring. This autumn increase on the North Slope, together with the fact that the largest increases are in northern and western Alaska during winter, points to a role of sea ice in amplifying the warming. The later freeze-up and thinner winter ice cover are conducive to large ocean-to-atmosphere heat fluxes during late autumn and winter, and these fluxes impact air temperatures in the coastal regions adjacent to the Bering, Chukchi and Beaufort Seas. The extremely large temperature anomaly and excess warmth at Barrow in Fig. 5 is a specific example of the impact of diminished sea ice on coastal temperatures.

The fact that the increase of excess warmth is greater in spring than in autumn over the climate divisions south of the Brooks range points to a role of snow cover, specifically the earlier snow disappearance that enables a jump in absorbed solar radiation, as illustrated for the 2016–17 winter by Walsh et al. (2017). Because incoming solar radiation is much weaker in September–November (autumn) than in March–May (spring), one would expect a smaller contribution to excess warmth from later snow-on dates than from earlier snow-off dates, consistent with Fig. 9.

4. Discussion

Given the increases in “excess warmth” summarized above, we now

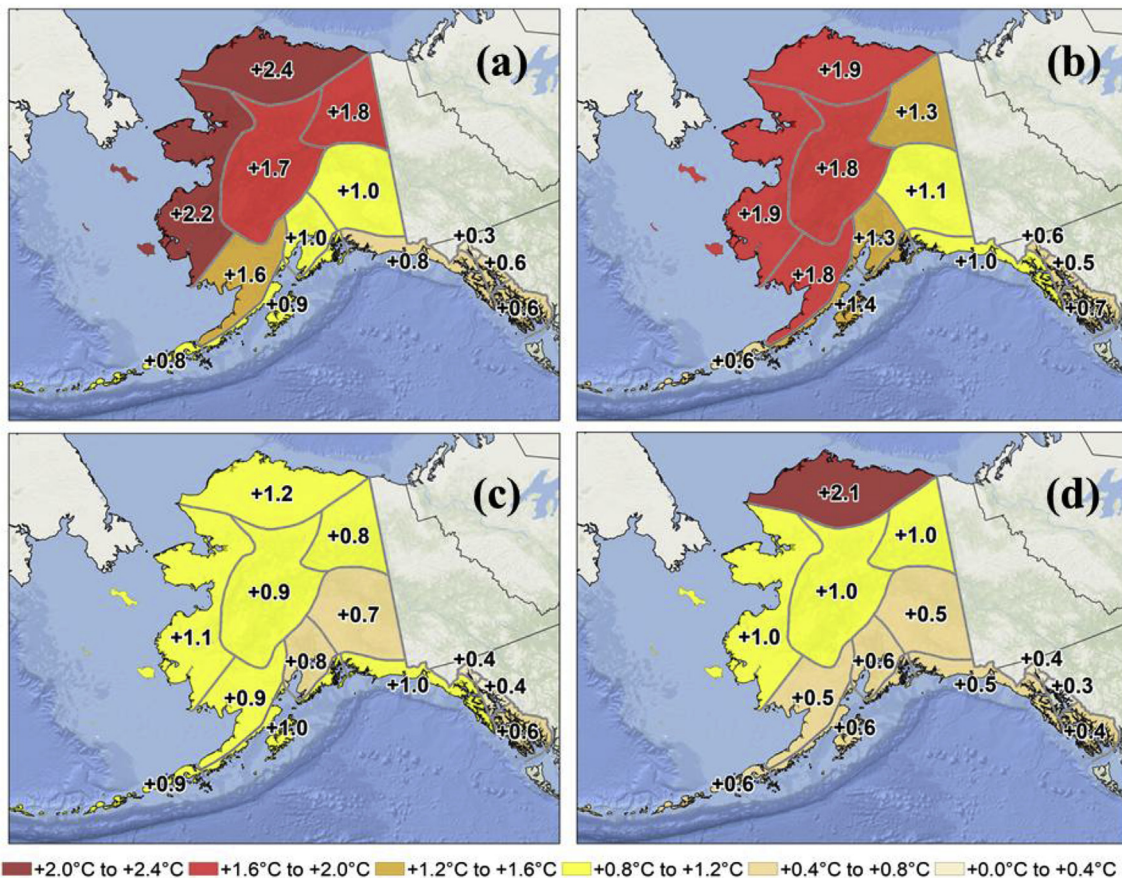


Fig. 9. Change in excess warmth (°C) during 1950–2017 as a function of Alaska climate division in each of the four seasons: (a) winter, Dec–Feb, (b) spring, Mar–May, (c) summer, Jun–Aug, and (d) autumn, Sep–Nov. Brown and red denote largest changes (see color legend at bottom). (For interpretation of the references to color in this figure legend, the reader is referred to the Web version of this article.)

return to the interpretation in terms of increased external forcing by greenhouse gases (GHGs). Global climate models have provided historical and 21st-century simulations with observed GHG forcing under various prescribed scenarios of GHG forcing. The most extensive compilation of output from these simulations is available through the Coupled Model Intercomparison Project, CMIP, for which versions 3 and 5 have been used in the two most recent assessments by the Intergovernmental Panel on Climate Change (IPCC 2007; 2013). For comparison with our observationally-based analysis, we utilize two evaluations of the CMIP simulations for the Arctic over the 1950–2017 time frame used in the present study (including the hemispheric depiction in Fig. 1). Overland et al. (2018) have composited the winter (Dec–Feb) and annual temperatures simulated for the Arctic (60°–90°N) by an ensemble of 36 CMIP5 models. The ensemble mean warming over the 1950–2017 period is 1.8 °C for the annual temperatures and 2.6 °C for the winter temperatures (Overland et al., 2018, their Fig. 3). Both are consistent with the observed warmings (averaged over the polar cap) in Fig. 1. However, the comparison with the CMIP models is not clean because the CMIP averages are Arctic-wide rather than Alaska-specific. An earlier study by Hodson et al. (2013) showed time series of mean annual temperatures simulated by the CMIP3 models for the Arctic (70°–90°N). The mean change of the 21 models composited by Hodson et al. in their Fig. 2 is 1.7 °C from the early 1950s to 2017, essentially the same Arctic warming shown by Overland based on their CMIP5 composite.

Because the model-derived temperature changes summarized above are composites from (35 and 21) global models, the effects of internal variability are essentially removed by the averaging. This leaves the signal of GHG forcing in the difference fields and the effects of systematic errors in the suite of CMIP models. If one assumes that the systematic errors of the different models largely offset so that errors in the ensemble means of the future simulations are small (as they are in the historical simulations), then the GHG warming since 1950 is approximately 1.8 °C annually and 2.6 °C in winter. The results of Section 3 show that the “excess warmth” is approximately 1.5 °C in the annual mean and 2.1 °C in winter. It is apparent that the excess warmth is very consistent with the effects of increased GHG forcing simulated by the ensembles of global climate models. This consistency applies not only to the annual mean but to the seasonality in the sense that both the excess warmth and the GHG warming are larger in winter than in the other seasons and in the annual mean.

An underlying premise of this paper is that the dynamically forced component of the temperature variability and trend represents internal variability. However, this assumption is open to question to the extent that greenhouse forcing affects the atmospheric circulation. In the context of the present study, a key feature of the atmospheric circulation is the Aleutian low, which was shown earlier (Fig. 4) to drive large year-to-year variations of Alaska's temperatures. There is emerging evidence that anthropogenic warming contributes to a strengthening of the Aleutian low (Zhang and Delworth, 2007; Wu et al., 2008; Gan et al., 2017). However, models show considerable spread in their greenhouse-driven changes of the atmospheric circulation in the North Pacific, and the historical decrease of pressure in the Aleutian region has exceeded that simulated by climate models run with historical greenhouse forcing (Gillett et al., 2003; Gan et al., 2017), suggesting that internal variability has played a role in trends of the Aleutian low over the past 50–100 years. We also note that the study periods utilized in the historical trend assessments by Gillett et al. and Zhang et al. do not coincide with the 1950–2017 period used here. .

5. Conclusion

The results obtained here show that (1) the atmospheric circulation explains a substantial portion of the winter and autumn variability and trends of temperature over Alaska, and (2) the portion of the temperature variations unexplained by the atmospheric circulation exhibits

a systematic trend in all seasons over the 1950–2017 period. If the portion of the variations not explained by the circulation is termed “excess warmth”, the excess warmth accounts for about 1.5 °C of the total 2.1 °C warming of the annual mean temperature since 1950. This contribution is largest (2.1 °C) in winter and spring, the two seasons in which the observed warming has been largest, and it compares favorably with the model-simulated warming attributable to increased greenhouse gas forcing. According to our observational results, the excess warmth represents 51% of the total warming of 4.2 °C during winter and 75% of the total warming of the annual mean of Alaska's statewide temperature since 1950.

As noted in Section 2, the approach used in this study cannot distinguish the direct radiative effect of increasing GHG concentrations from the effects of varying surface conditions (ocean temperatures, sea ice, snow cover), for which changes may be driven at least in part by increasing GHG concentrations. Similarly, the present approach cannot distinguish radiative impacts of anthropogenic greenhouse gas increases (CO₂, CH₄) from associated increases of water vapor and its associated downwelling longwave radiation. Variations in the atmospheric circulation also play a role in the cloud cover, which can affect surface air temperatures in all seasons. Controlled model experiments are required to sort out the effects of these various components of anthropogenic forcing. However, the results reported here do point to the importance of the atmospheric circulation in explaining the recent warming of Alaska during winter and autumn, when the atmospheric circulation explains 49% and 25% of the warming, respectively. By contrast, the atmospheric circulation has not made a detectable contribution to changes of temperature over Alaska during spring and summer.

Finally, the analog methodology cannot address the possibility that GHG forcing may be contributing to changes in the atmospheric circulation. However, there is an emerging consensus that systematic changes of the atmospheric circulation in middle and high latitudes are presently obscured by internal variability (Shepherd, 2014; Screen et al., 2014; Overland, 2016). Deser et al. (2016) also concluded that the component of the temperature trends forced by changes in the atmospheric circulation has been small over recent decades, although Saffioti et al. (2017) indicate that it may not be negligible in the future. The fact that greenhouse forcing can drive model-derived trends of circulation in the Alaska region (e.g., Gillett et al., 2003; Gan et al., 2017) points to the need for controlled model experiments to disentangle the effects of greenhouse forcing and internal variability on temperatures in Alaska, especially with regard to future changes.

Acknowledgements

This work was supported by the Climate Program Office of the National Oceanic and Atmospheric Administration through Grants NA15OAR4310169 and NA16OAR4310162. We thank Peter Bieniek for assistance with the graphics.

Appendix A. Supplementary data

Supplementary data to this article can be found online at <https://doi.org/10.1016/j.polar.2018.09.002>.

References

- Bieniek, P.A., Bhatt, U.S., Thoman, R.L., Angeloff, H., Partain, J., Papineau, J., Fritsch, F., Holloway, E., Walsh, J.E., Daly, C., Shulski, M., Hufford, G., Hill, D.F., Calos, S., Gens, R., 2012. Climate divisions for Alaska based on objective methods. *J. Appl. Meteorol. Climatol.* 51, 1276–1289.
- Cattiaux, J., Vautard, R., Cassou, C., Yiou, P., Masson-Delmotte, V., Codron, F., 2010. Winter 2010 in Europe: a cold extreme in a warming climate. *Geophys. Res. Lett.* 37 <https://doi.org/10.1029/2010GL044613>. L20704.
- Cullather, R.L., Lim, Y.-K., Boisvert, L.N., Brucker, L., Lee, J.N., Nowicki, S.M.J., 2016. Analysis of the warmest Arctic winter, 2015–2016. *Geophys. Res. Lett.* 43 (10), 808–810. <https://doi.org/10.1002/2016GL071228>. 816.

- Deser, C., Phillips, A.S., Alexander, M.A., Smoliak, B.V., 2014. Projecting North American climate over the next 50 years: uncertainty due to internal variability. *J. Clim.* 27, 2271–2296.
- Deser, C., Terray, L., Phillips, A.S., 2016. Forced and interannual components of winter air temperature trends over North America during the past 50 years: mechanisms and implications. *J. Clim.* 29, 2237–2258.
- Gan, B., Wu, L., Jia, F., Li, S., Cai, W., Nakamura, H., Alexander, M.A., Miller, A.J., 2017. On the response of the Aleutian low to greenhouse warming. *J. Clim.* 30, 3907–3925.
- Gillett, N.P., Zwiers, F.W., Weaver, A.J., Stott, P.A., 2003. Detection of human influence on sea level pressure. *Nature* 422, 292–294.
- Hartmann, B., Wendler, G., 2005. The significance of the 1976 Pacific climate shift in the climatology of Alaska. *J. Clim.* 18, 4824–4839.
- Hodson, D.L.R., Keeley, S.P.E., West, A., Ridley, J., Hawkins, E., Hewitt, H.T., 2013. Identifying uncertainties in Arctic climate projections. *Clim. Dynam.* 40, 2849–2865.
- IPCC, 2013. Climate change 2013. In: Stocker, T.F., Qin, D., Plattner, G.-K., Tignor, M., Allen, S.K., Boschung, J., Nauels, A., Xia, Y., Bex, V., Midgley, P.M. (Eds.), *The Physical Science Basis. Contribution of Working Group I to the Fifth Assessment Report of the Intergovernmental Panel on Climate Change*. Cambridge University Press, Cambridge, UK, pp. 1535.
- IPCC, 2007. Climate change 2007. In: Solomon, S., Qin, D., Manning, M., Chen, Z., Marquis, M., Averyt, K.B., Tignor, M., Miller, H.L. (Eds.), *The Physical Science Basis. Contribution of Working Group I to the Fourth Assessment Report of the Intergovernmental Panel on Climate Change*. Cambridge University Press, Cambridge, UK, pp. 996.
- Kalnay, E., et al., 1999. The NCEP/NCAR 40-year reanalysis project. *Bull. Am. Meteorol. Soc.* 77, 437–471.
- Lehner, F., Deser, C., Terray, L., 2017. Toward a new estimate of “time of emergence” of anthropogenic warming: insights from dynamical adjustment and a large initial-condition model ensemble. *J. Clim.* 30, 7739–7756.
- Lorenz, E.N., 1969. Atmospheric predictability as revealed by naturally occurring analogs. *J. Atmos. Sci.* 26, 636–646.
- McAfee, S.A., 2014. Consistency and lack thereof in Pacific decadal oscillation impacts on North American winter climate. *J. Clim.* 27, 7410–7421.
- Mills, C.M., Walsh, J.E., 2013. Seasonal variation and spatial patterns of the atmospheric component of the Pacific Decadal Oscillation. *J. Clim.* 26, 1575–1594.
- Overland, J.E., 2016. A difficult Arctic science issue: midlatitude weather linkages. *Polar Sci.* 10, 210–216.
- Overland, J.E., Dunlea, E., Armstrong, T., Box, J.E., Corell, R., Forsius, M., Kattsov, V., Olsen, M.S., Pawlak, J., Reiersen, L.-O., Wang, M., 2018. The immediacy of Arctic change. *Polar Sci* in press.
- Papineau, J.M., 2001. Wintertime temperature anomalies in Alaska correlated with ENSO and the PDO. *Int. J. Climatol.* 21, 1577–1592.
- Pithan, F., Mauritsen, 2014. Arctic amplification dominated by temperature feedbacks in contemporary climate models. *Nat. Geosci.* 7, 181–184.
- Richter-Menge, J., Mathis, J.T., 2017. The arctic. In state of the climate in 2016. *Bull. Am. Meteorol. Soc.* 98 (8 Special Suppl.), S129–S154.
- Saffioti, C., Fischer, E.M., Knutti, R., 2017. Improved consistency of climate projections over Europe after accounting for atmospheric circulation variability. *J. Clim.* 30, 7271–7291.
- Screen, J.A., Deser, C., Simmonds, I., Tomas, R., 2014. Atmospheric impacts of Arctic sea ice loss, 1979–2009: separating forced change from internal variability. *Clim. Dynam.* 43, 333–344.
- Serreze, M.C., Barrett, A.P., Stroeve, J., 2012. Recent changes in tropospheric water vapor over the Arctic as assessed from radiosondes and atmospheric reanalyses. *J. Geophys. Res.* 117 <https://doi.org/10.1029/2011JD017421>. D10104.
- Shepherd, T.G., 2014. Atmospheric circulation as a source of uncertainty in climate change projections. *Nat. Geosci.* 7, 703–708. <https://doi.org/10.1038/ngeo2253>.
- Shulski, M., Wendler, G., 2007. *The Climate of Alaska*. University of Alaska Press, pp. 208.
- Smoliak, B.V., Wallace, J.M., Lin, P., Fu, Q., 2015. Dynamical adjustment of Northern Hemisphere surface air temperature field: methodology and application to observations. *J. Clim.* 28, 1613–1629.
- SWIPA, 2011. Snow, water, ice and permafrost in the arctic: climate change and the cryosphere. In: *Arctic Monitoring and Assessment Programme (AMAP)*, Oslo, Norway, pp. 538.
- Van den Dool, H.M., Huang, J., Fan, Y., 2003. Performance and analysis of the constructed analogue method applied to U.S. soil moisture over 1981–2001. *J. Geophys. Res.* 108, 8617. <https://doi.org/10.1029/2002/D003114>.
- Walsh, J.E., Bieniek, P.A., Brettschneider, B., Euskirchen, E.S., Lader, R., Thoman, R.L., 2017. The exceptionally warm winter of 2015–16 in Alaska. *J. Clim.* 30, 2069–2088.
- Wu, L., Li, C., Yang, C., Xie, S.-P., 2008. Global teleconnections in response to a shutdown of the Atlantic meridional overturning circulation. *J. Clim.* 21 3002–2019.
- Zhang, R., Delworth, T.L., 2007. Impact of the Atlantic multidecadal oscillation on North Pacific climate variability. *Geophys. Res. Lett.* 34 <https://doi.org/10.1029/2007GL031601>. L23709.